# SEABED PARAMETER ESTIMATION BY INVERSION OF LONG RANGE SOUND PROPAGATION FIELDS

WEI CHEN, LI MA

*Institute of Acoustics, Chinese Academy of Sciences, Beijing*

N. ROSS CHAPMAN

*University of Victoria, Victoria, BC, Canada*

**Abstract**- The seabed parameters are especially important in underwater sound propagation in shallow water. A long range geoacoustic inversion experiment was conducted in January 2005, in winter conditions in the South China Sea where the bottom is mostly sand and silt. In this experiment, single frequency CW pulse signals were transmitted from a suspended source, and received by a vertical array of hydrophones. The data were inverted for the geoacoustic properties of the seabed using a hybrid inversion method—the adaptive simplex simulated annealing (ASSA). Owing to the identical inversion procedures, the favorable results were obtained for 6 unknown geometrical and geoacoustic parameters by the semi-infinite seabed model. It is shown that seabed inversion parameters are consistent for the different time arrival signals. By comparing with the inversion for a sediment over basement bottom model, the single layer seabed geoacoustic model is adequate to obtain the equivalent seabed parameters very well for the long range experiment site.

## I. INTRODUCTION

Ocean acoustic inversion methods based on Matched Field Processing (MFP)[1] can be applied to estimate properties of the seabed. MFP inversions use numerical simulations to model the acoustic response to different seabed types and efficient search optimization algorithms to find the environment parameters that give the best agreement between the modeled and measured data. Typically, MFP inversions use acoustic data received on a vertical array with many hydrophones and a sound source in a fixed location. In the past several years, the feasibility of MFP inversion has been shown in both simulation and experiment[2-5].

In this paper, results of MFP inversions are presented for sets of pulsed CW data from a long range acoustic propagation experiment. Inversion performance is compared for two geoacoustic models; first, a semi-infinite seabed goeacoustic model, and then, a sediment layer over a semi-infinite basement model.

## II. THE LONG RANGE GEOACOUSTIC INVERSION EXPERIMENTS

The sound propagation experiments were conducted in January, 2005, off the southwest coast of Hanan Island in the South China Sea. An acoustic source at 17°29′ N 109°36′E was suspended at approximately 30 m depth from a research vessel. The propagation distance was about 43 km as shown in Figure 1. Pulsed CW signals of 1-s pulse duration were transmitted at 650 Hz. The signals were recorded on a vertical array of hydrophones (VLA). The VLA was centered at mid-water depth from 7 m to 69 m suspended from another boat. The array contained 32 hydrophones equally spaced at 2 m. The data considered here were taken in less than 1 hour.

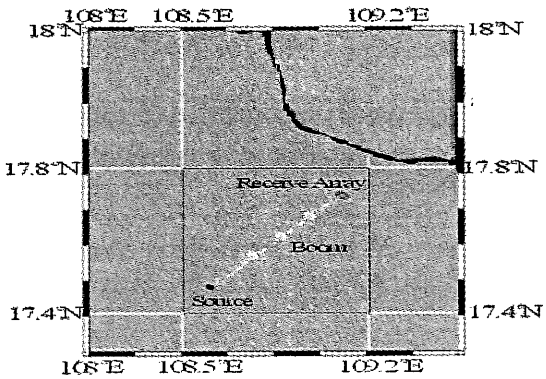


Fig. 1. Long range inversion experimental area showing the source and vertical array positions.

The stationary sound speed profiles in the water were determined from conductivity temperature-depth (CTD) measurements. The sound speed in water layer varied little from 1529.2 m/s to 1530.3 m/s, as shown in the two sound speed profiles in Fig. 2. The very weak gradient is due to the nearly constant sea water temperature in the winter season. In this experiment, the signal strength of the 650-Hz CW pulse signal was strong (signal-to-noise ratio about 8 dB) at the distance of 43 km. Several pulses were recorded for geoacoustic inversion, as shown in Fig. 3, and three were used separately for geoacoustic inversion.

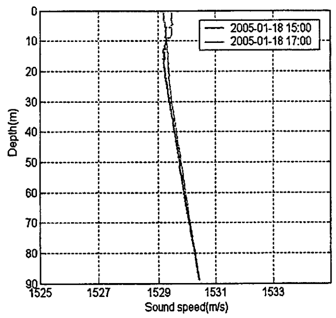


Fig. 2. The stationary sound speed profiles.

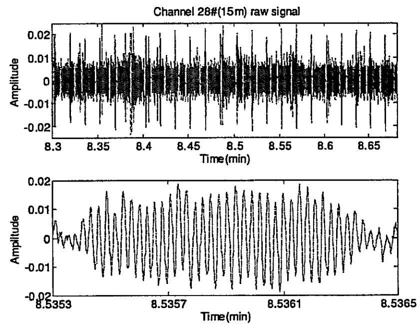


Fig. 3. 650-Hz CW Pulse signal received by the 28th hydrophone of the VLA at 43 km range.

## III. GEO-ACOUSTIC INVERSION METHOD

The geoacoustic inversion process for estimating the seabed properties consists of the following:

- Assume a reasonable geoacoustic model to describe the interaction with the sea bottom.
- Select a numerical propagation method to compute the forward acoustic field.
- Consider an appropriate objective function as a criterion to quantify the agreement between measured and simulated data.
- Select an efficient optimization algorithm to search for the set of environmental parameters which produces the lowest objective function value.

A. The geo-acoustic model

We consider two kinds of geoacoustic models for the long-range inversion. First, a water layer over fluid half-space seabed is chosen, (Model 1). In this model six parameters are unknown, including three geometric parameters (water depth, D, source range and depth, r and z), and three geoacoustic parameters of the bottom: compressional speed c, density ρ and attenuation α. A fluid thin layer over the half-space bottom was also used for a geoacoustic model, i.e., Model 2. In this model the sound speed in the sediment is assumed to vary linearly with depth, whereas it is taken to be depth independent in the half-space bottom. The density and attenuation are assumed depth independent within each layer. Eleven parameters are unknown, as shown in Fig 4 (right). For inversions of the long-range experimental data, Table 1 lists each of the unknown parameters and their search intervals. The ocean sound speed profile and sensor positions were considered known in the inversions with both models.

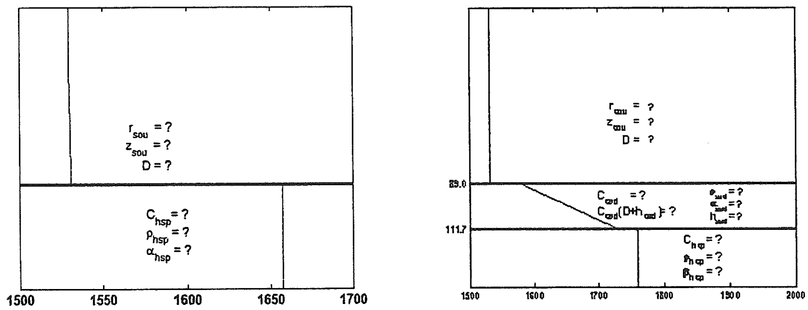


Fig. 4 Two kinds of geoacoustic models, Model 1 (left) and Model 2 (right).

Table 1. Inversion parameters, labels and search intervals in Semi-infinite Seabed Model 1.

| Parameters Description | Label | Search Interval |
|---|---|---|
| Source range (km) | $r_{sou}$ | 40-46 |
| Source depth (m) | $z_{sou}$ | 20-40 |
| Water depth change (m) | D | 80-100 |
| Sediment speed (m/s) | $c_{sed}$ | 1600-1800 |
| Sediment attenuation (dB/λ) | $\alpha_{sed}$ | 1.4-2.0 |
| Sediment density ( $g/m^3$ ) | $\rho_{sed}$ | 0.05-1 |

Table 2. Inversion parameters, labels and search intervals in two-layered Seabed Model 2.

| Parameters Description | Label | Search Interval |
|---|---|---|
| Source range (km) | $r_{sou}$ | 40-46 |
| Source depth (m) | $z_{sou}$ | 20-40 |
| Water depth change (m) | D | 80-100 |
| Sediment speed (m/s) | $c_{sed}$ | 1500-1600 |
| Sediment speed bottom (m/s) | $c_{sed}(D+h_{sed})$ | 1600-1800 |
| Sediment thickness (m) | $h_{sed}$ | 2-30 |
| Sediment attenuation (dB/λ) | $\alpha_{sed}$ | 0.05-1 |
| Sediment density ( $g/m^3$ ) | $\rho_{sed}$ | 1.4-1.85 |
| Basement speed (m/s) | $c_{hsp}$ | 1600-1800 |
| Basement attenuation (dB/λ) | $\alpha_{hsp}$ | 0.05-1 |
| Basement density ( $g/m^3$ ) | $\rho_{hsp}$ | 1.7-2.1 |

**B.** The forward propagation model

The forward propagation model used to compute the replica pressure fields was the normal-mode model KRAKENC[6].

C. The objective function

The objective function, *E*, which is minimized by the search algorithm, consists of the normalized Bartlett processor mismatch

$$E(m) = 1 - \frac{\left|p^* \cdot p(m)\right|^2}{\left|p\right|^2 \left|p(m)\right|^2}$$

where p represents the measured acoustic field data (complex acoustic pressure) and p(m) is the modeled or replica field. The model vector $\boldsymbol{m}=\{m_i\}$, $i=1,2,\ldots n$. The symbol * indicates the complex conjugation operation. This objective function *E* is normalized and always produces $0 < E < 1$ (where a perfect match yields $E = 0$).

**D.** The search algorithm

In this paper, an adaptive simplex simulated annealing (ASSA) algorithm is used for the inversions. The ASSA algorithm combines simulated annealing (SA) and the downhill simplex method (DHS) in an adaptive manner. SA is a global search involving random perturbations of the unknown model parameters. However, random perturbations that neglect gradient information are inefficient for correlated parameter spaces. Alternatively, the DHS method is a local method that retains a memory of the best models encountered in its search; combining this method with SA in a hybrid algorithm effectively provides the required memory. The result is that, as a hybrid inversion ASSA is both simpler and significantly more efficient and effective than an earlier, non-adaptive version of the algorithm. More detail about the ASSA algorithm is reported by Dosso et al.[7]

## IV. INVERSION RESULTS

The sound field data from three CW pulse signals: No. 9 pulse, No. 16 pulse and No. 26 pulse, were used in the inversions. The estimated values of the six unknown parameters for the semi-infinite seabed model are listed in Table 3. The estimated values of each pulse inversion are very similar to those of the other two, except the attenuation coefficient of the second pulse The estimate for source range is in excellent agreement with the measured value of 43 km that was determined in the experiment using a differential global positioning system. Source depth was estimated with an accuracy less than 5 m of the true source depth (verified by a depth sensor TD on the source body). The sea maps showing the seabed type indicate a surface sand layer throughout the experimental area. The inverted values for the geoacoustic properties of the sediment are consistent with those for a silty sand type bottom reported by Hamilton.[8]

An example of the annealing process is illustrated in Fig. 5. The annealing schedule consisted of an initial temperature of 0.3 and a temperature reduction factor of 0.99, with five perturbations at each of the approximately 36000 temperature steps prior to quenching. Stable estimates are obtained for all parameters, including the low-sensitive parameters such as density and attenuation. The high-sensitive geometric parameters, source range and depth, are determined to a low-energy near the known (true) values very early in the annealing process. Fig. 6 shows the one-dimensional (1-D) cross sections of the parameter space. In each panel, the other parameters that are not varied are held fixed at their final values. This figure illustrates the features that make geoacoustic inversion a challenging problem: the 1-D cross sections exhibit multiple local minima, in this case for some of the sensitive geometrical parameters. Fig. 6 displays a wide range in parameter sensitivities (a sensitive parameter is one for which a small change in the parameter value near the minimum results in a large change in the mismatch). Source range and depth (r,z) and water depth D are the most sensitive parameters, while the others are less sensitive. Parameter sensitivities determined in this manner are commonly used to identify which parameters can be well determined by inversion. However, it should be recognized that 1-D sensitivities provide an incomplete description of the parameter space since they ignore multi-dimensional correlations.

Table 3. Geoacoustic and Geometrical parameter estimates for the inversion at source range 43 km.

| | $C_{hsp}$ (m/s) | $\rho_{hsp}$ ($g/m^3$) | $\alpha_{hsp}$ ($dB/\lambda$) | $r_{src}$ (km) | $z_{src}$ (m) | D(m) |
|---|---|---|---|---|---|---|
| Pulse 09 | 1668.83 | 1.761 | 0.839 | 43.199 | 25.372 | 83.539 |
| Pulse 16 | 1658.08 | 1.841 | 0.493 | 43.529 | 24.382 | 83.409 |
| Pulse 26 | 1677.15 | 1.669 | 0.644 | 42.846 | 23.869 | 82.928 |

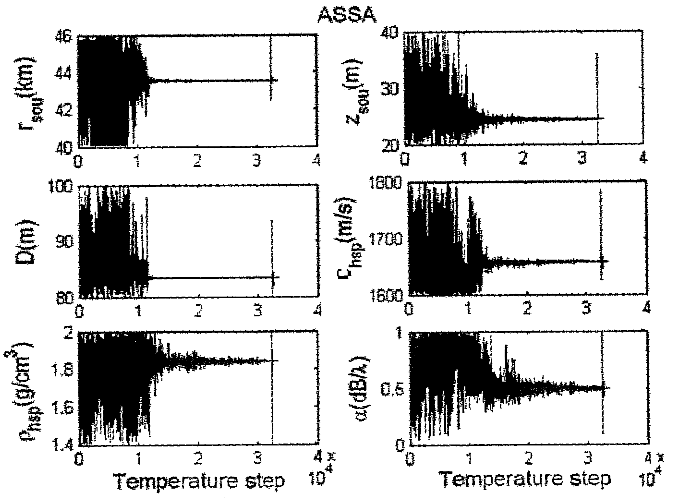


Fig.5 The annealing process of the each estimated parameter from ASSA inversion.

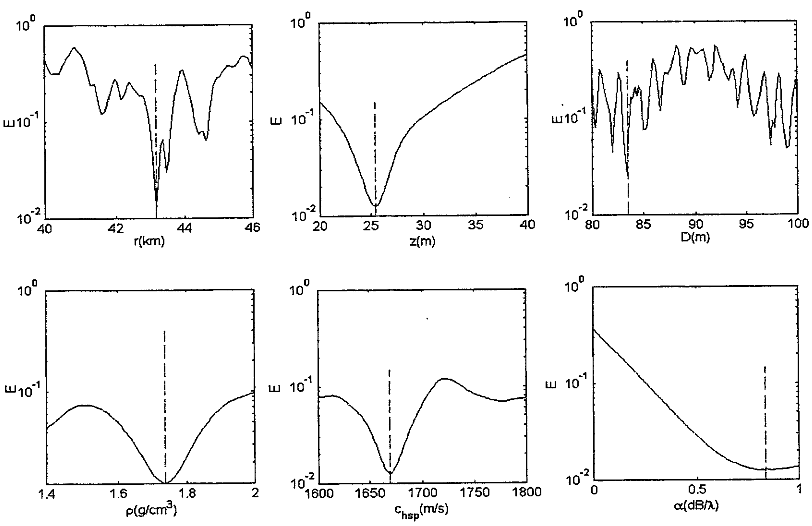


Fig. 6. 1-D cross sections of the parameter space for the model 1.

A more practical approach to describe the multi-dimensional sensitivity of the parameters, as a by-product of the ASSA inversion, is illustrated in Fig. 7. The panels in the figure display the mismatch E of each accepted model as a function of the individual model parameters. This has the advantage of including parameter sampling over the multi-dimensional space. It is interesting to note that according to the multi-dimensional analysis in Fig. 7, the sensitivities of parameters (r ,z) and D are substantially reduced compared to the 1-D analysis, likely as a result of the strong correlation between these parameters.

An example of the annealing process for the two layer seabed is shown in Fig. 8. The geometric parameters are the most sensitive, with the sediment layer and basement half space parameters in descending order of sensitivity. The estimated values for the sensitive geometric parameters are in good agreement with the values obtained in the experiment. Comparing the estimated values for the geoacoustic parameters from the inversions with both models, we note that the estimated sediment sound speed for model 1 is roughly a mean value of the estimated sound speeds for the sediment and basement half space from Model 2.

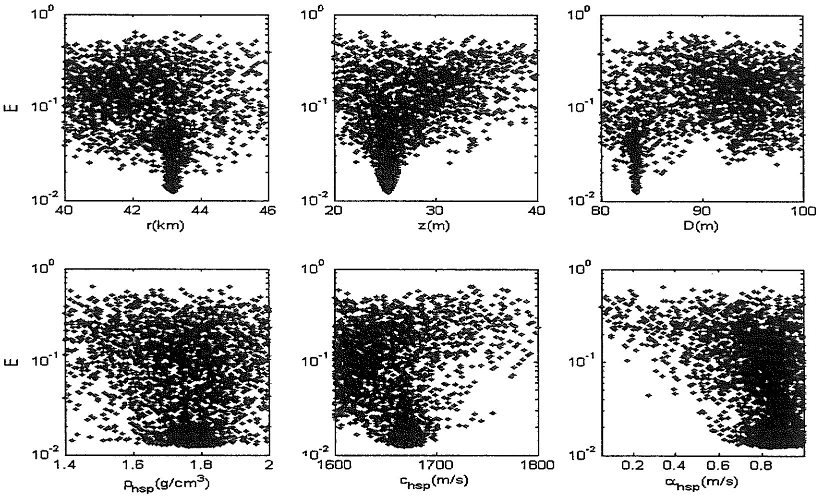


Fig. 7. Multi-dimensional sensitivity analysis. The small dots indicate the mismatch as a function of parameter values from ASSA inversion.

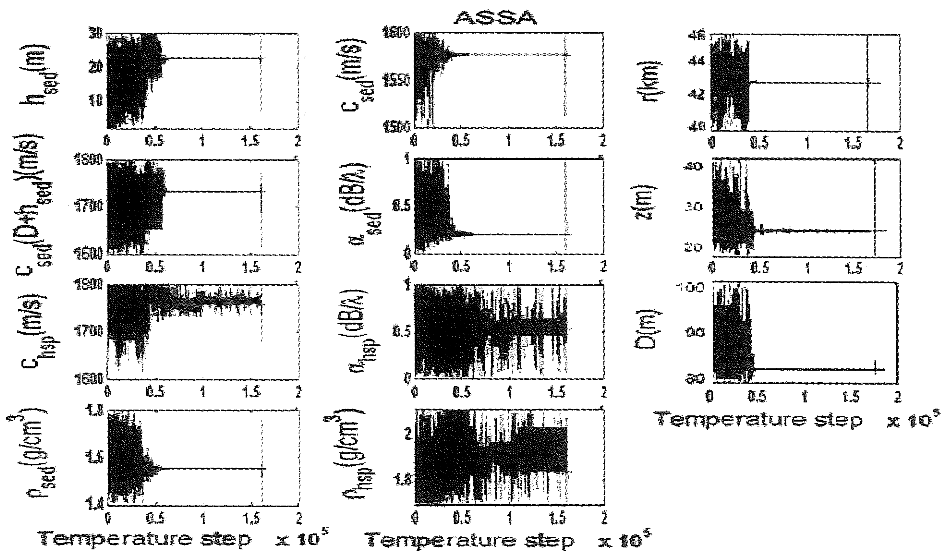


Fig. 8. The estimated parameters of Model 2 using the ASSA inversion.

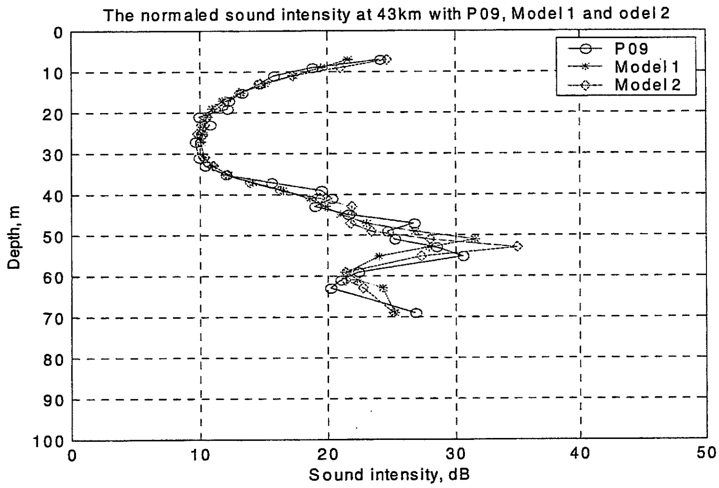


Fig 9. Comparison between measured (solid) and modeled (dashed) pressure field magnitudes as a function of depth. Measured field magnitudes are normalized to the modeled field levels.

## V. DISCUSSION AND CONCLUSIONS

The fit to the experimental pressure field at the array for calculated fields based on the inverted models is shown in Fig. 9. Although both models can fit the data very well, the ASSA inversions suggest that the data are sensitive mostly to the sea floor sediment parameters, and not sensitive to the deeper layers. This comparison indicates that a simple sea bed half-space model is sufficient for describing the interaction with the sea bottom. Moreover, the estimated values of the sea floor sediments are in good agreement with the expected values for the sandy sediment material at the experimental location.

The geometrical parameters strongly influenced the objective function value and sometimes dominated the inversion. Improved results were obtained using a three-step process to search for the geometrical and geoacoustic parameters. The complete process took about 3 and half hours on a Intel4 processor.


## Acknowledgments

We would like to thank Yaoming CHEN for drawing the figure of the sound field.


## References


[1] A. Tolstoy, Matched Field Processing for Underwater Acoustics, London, U.K. World Scientific, 1993.

[2] T C. Yang and C W. Bogart, Matched mode processing for sparse three-dimension arrays, J. Acoust. Soc. Am. 95(6), 3149–3166, 1994.

[3] J-P Hermand and P. Gerstoft, Inversion of broadband multitone acoustic data from the Yellow Shark experiment, IEEE J. Ocean. Eng., vol. 21, No. 3, 324-346, 1996.

[4] L. Jaschke and N.R. Chapman, Matched field inversion of broadband data using the freeze bath method, J. Acoust. Soc. Amer., 106, 1838-1851, 1999.

[5] M. Siderius, P. Nielsen and P. Gerstoft, Range dependent sea bed characterization by inversion of acoustic data from a towed array receiver, J. Acoust. Soc. Amer., 112, 1523-1535, 2002.

[6] M.B. Porter, The KRAKEN normal mode program, SACLANTCEN Technical Report SM-245, SACLANT Undersea Research Centre, La Spezia Italy, 1991.

[7] S E. Dosso, M J. Wilmut, A S. Lapinski, An Adaptive-Hybrid Algorithm for Geoacoustic Inversion, IEEE J. Ocean. Eng., vol. 26, No. 3, 324-336, 2001.

[8] Hamilton E L. Compressional-wave attenuation in marine sediments. Geophysics, 37, 620, 1972.